JOURNAL OF APPLIED ELECTROCHEMISTRY 22 (1992) 1049–1054

Lanthanum phosphate-bonded composite nickel electrodes for alkaline water electrolysis

H. DUMONT, P. W. WRONA*, J. M. LALANCETTE, H. MÉNARD*

Département de Chimie, Université de Sherbrooke, Sherbrooke, Québec, Canada J1K 2R1

L. BROSSARD

Institut de Recherche d'Hydro-Québec (IREQ), 1800 montée Ste-Julie, Varennes, Québec, Canada J3X 1S0

Received 10 May 1991; revised 12 October 1991

Nickel-powder electrodes bonded with a polymer of lanthanum phosphate were prepared and tested for their performance in water electrolysis of KOH aqueous solutions. Disintegration of the phosphate-bonded electrodes made with spiky filamentary nickel particles is strongly reduced at open circuit potential with $LaPO_4$ rather than $AlPO_4$ as the binding material, but the electrocatalytic performance toward hydrogen evolution is practically the same for both materials.

1. Introduction

Industrial water electrolysis calls for stable performance and low hydrogen and oxygen overpotentials. Nickel-based electrodes are known to be among the most active electrocatalysts in hot concentrated alkaline solutions [1–4]. Recently, however, a new technique for cementing metallic powders to produce high surface area nickel electrodes has been reported [5] with the advantage that it does not need a reducing atmosphere. The metallic particles are shaped into useful electrodes by binding them under pressure with a polymer of aluminum phosphate, $AlPO_4$.

However, $AlPO_4$ is unstable in the presence of hot concentrated alkaline solutions with the result that electrodes containing spheroidal, nodular or cauliflower-like particles of nickel are destroyed in 30 wt % NaOH at 70° C after several minutes of immersion. The best chemical stability and performance for the hydrogen evolution reaction (HER) in such conditions are obtained with 98 wt % spiky filamentary nickel particles containing 2 wt % $AlPO_4$.

The present investigation deals with nickel electrodes made with a new binder, a polymer of lanthanum phosphate. It is shown that the latter compound is very stable in hot concentrated alkaline solutions compared to aluminum phosphate. Consequently, disintegration of phosphate-bonded electrodes made with spiky filamentary nickel particles is considerably less when $LaPO_4$ is used. The HER and the oxygen evolution reaction (OER) of such electrodes as a result of the electroreduction of water in KOH are also considered.

2. Experimental details

2.1. *Preparation*

2.1.1. The binder. Lanthanum phosphate was produced by combining acid lanthanum phosphate and lanthanum hydroxide. Two overall reactions are involved in the formation of acid phosphate lanthanum $La(H_2PO_4)_3$ and its subsequent transformation into $LaPO_4$:

$$\tfrac{1}{2}La_2O_3 + 3H_3PO_4 \longrightarrow La(H_2PO_4)_3 + \tfrac{3}{2}H_2O \quad (1)$$

$$La(H_2PO_4)_3 + 2La(OH)_3 \longrightarrow 3LaPO_4 + 6H_2O \quad (2)$$

The $La(H_2PO_4)_3$ was synthesized by adding 48.88 g (0.15 mol) La_2O_3 to 103.7 g (0.90 mol) H_3PO_4 (85%) in a rectangular Teflon cell measuring 10 cm × 5 cm × 5 cm. (Teflon was used because a reactive intermediate may react with glass.) The reactive mixture was stirred constantly during the addition of La_2O_3 until a very thick, silicone-like paste was obtained. Since the reaction was very fast, strongly exothermic and autocatalytic, even when the components were mixed at room temperature, the La_2O_3 should be completely incorporated within a few minutes. As soon as the reaction ended, the Teflon reactor was heated in an oven at 150° C for 24 h. The reaction product, in the form of a viscous paste, was then transferred to a flask and vacuum dried to remove traces of water produced during the reaction. The addition of 0.883 g (0.005 mol) $La(OH)_3$ for 1 g (0.0025 mol) $La(H_2PO_4)_3$ made it easier to crush and mix the two components in a ball mill.

* On leave from Chemistry Department, University of Warsaw, 02093 Warsaw, Pasteura 1, Poland.

0021-891X

Since polymerization is very slow at room temperature, the mixture was stored for several days in a dessicator prior to final polymerization which was performed at 400° C for about 4 to 5 h.

2.1.2. The electrodes. A nickel powder of spiky filamentary particles (Inco 255) was obtained after sifting. A homogeneous mixture of $La(H_2PO_4)_3$ and $La(OH)_3$ was then added to a desired amount of nickel powder, and mixed thoroughly by hand. The electrodes were pressed under vacuum in a mould 1.3 cm in diameter, and nickel foil was introduced into the pellet to ensure proper electrical contact. After 12 h preheating at 150° C, polymerization was achieved by heating the pellets at 400° C for 4–5 h under a flow of argon. The electrodes were coated on one face and on the sides with Epofix resin (Struers) to obtain a 1.33 cm^2 (geometric) working surface area. Under these experimental conditions, it was observed that the morphology of nickel particles remained unchanged. When the polymerization was achieved at $T >$ 400° C, the needles on the spiky filamentary nickel particles tended to disappear and this was anticipated to be detrimental for the HER [6].

2.2. *Electrochemical measurements*

The experiments were performed in a two-compartment glass cell separated by a Dupont Nafion® membrane (Electrosynthesis Co.). The temperature of the cell compartment containing the working electrode was kept constant by circulating thermostated water. A Luggin capillary tube was placed less than 1 mm from the vertical working electrode. A nickel grid with a projected geometric surface area of 40 cm^2 was used as the counter electrode, while the reference was a Hg/HgO/1 M KOH electrode. The measured value of the reversible potential of the HER in 1 M KOH was −925 mV compared to the reference electrode. MilliQ water with 17.5 MΩ resistivity was used to prepare KOH solutions (Fisher-certified ACS reagent grade), which were deaerated by nitrogen bubbling. The current was applied by a galvanostat-potentiostat PAR 273 controlled by a Commodore PC2 microcomputer.

2.2.1. Kinetic parameters of the HER. Cathodic polarization curves were obtained by decreasing the applied current galvanostatically from 250 to 0.01 mA cm^{-2} after 30 min stabilization of the electrode potential at 250 mA cm^{-2}. The electrode potentials were corrected for the ohmic drop determined by a.c. impedance measurements. (Similar *IR* drop values were measured by current-interruption techniques [3].) Three sets of experiments were carried out. In the first set, $\log I$ against E curves were plotted for fresh electrodes, i.e. those with no chemical or electrochemical activation prior to cathodic polarization. In the second set, the nickel electrodes were electrochemically oxidized for 10 min at an anodic current of 250 mA cm^{-2} prior to hydrogen evolution. The last set of experiments was carried out after stabilization of the oxidized electrodes at a 250 mA cm^{-2} cathodic current. The two latter sets of experiments were carried out because it was shown that the hydrogen discharge on fresh Raney–Ni composite-coated electrodes may be largely influenced by the *in situ* electrochemical oxidation [4]. It was tentatively related to the formation of β $Ni(OH)_2$ and/or NiOOH during pre-oxidation.

2.2.2. HER overpotential against time. The potential against time curves for the HER were recorded in both 1 M KOH at a cathodic current density of 100 mA cm^{-2} and 30 wt % KOH at a current density of 150 mA cm^{-2} applied by a PAR potentiostat, model 173. The polarization time in KOH was 200 h. Since 2 wt % aluminium phosphate bonded nickel (APBN) electrodes and a 5 wt % lanthanum phosphate bonded nickel (LPBN) electrodes have the same molar percentage of phosphate polymer, their overpotential variation with time was compared.

2.2.3. Chemical stability at open circuit potential. LPBN electrodes containing 2, 10 and 20 wt % binding materials, respectively, were immersed in a 30 wt % NaOH solution at 70° C at open circuit potential (o.c.p.) and their weight loss after immersion was measured.

2.2.4. OER kinetic parameters. The Tafel parameters of the OER were obtained on LPBN electrodes in 1 M KOH at 25° C after two different polarization procedures. First, the kinetic parameters for different polarization times up to 48 h were determined for an anodic current of 250 mA cm^{-2}. In the second set of experiments, the measurements were performed at 25° C after 30 min of polarization at 70° C for different amounts of binding materials in the nickel electrodes.

In addition to the electrochemical characterization, the nature and morphology of electrode materials were investigated by scanning electron microscopy (SEM), X-ray diffraction (XRD), thermogravimetric analysis (TGA), energy dispersive X-ray microanalysis (EDX) and cyclic voltammetry (CV).

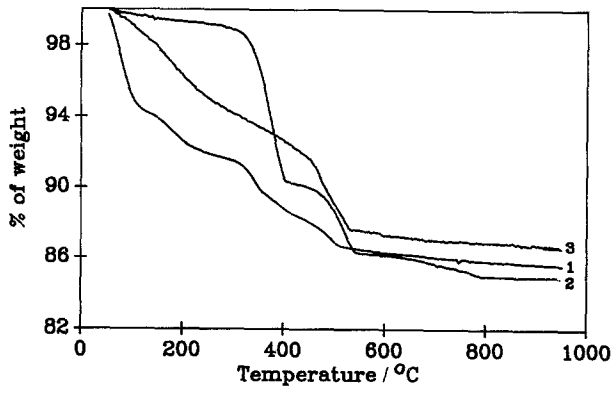

Fig. 1. Thermogravimetric analysis of polymerization. (1) $La(H_2PO_4)_3$ + $La(OH)_3$, (2) $La(OH)_3$, (3) $La(H_2PO_4)_3$.

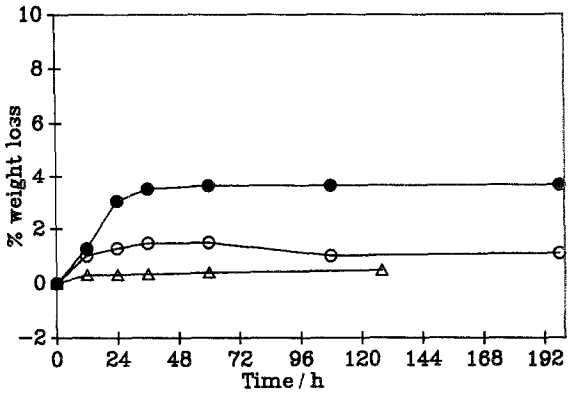

Fig. 2. Weight loss % of LPBN electrodes against time when immersed in 30 wt % NaOH at 70° C. Binder: (△) 2 wt %, (○) 10 wt %, and (●) 20 wt %.

3. Results and discussion

3.1. *Nature and morphology of the electrode materials*

TGA (Perkins Elmer) recordings are presented in Fig. 1. Curve 1 shows the dehydration of a mixture of 10 mg (0.023 mM) $La(H_2PO_4)_3$ and 8.85 mg (0.047 mM) $La(OH)_3$, which corresponds to the ratio of both compounds used in the polymerization process. It should be noted that the last dehydration step starts at about 400° C, which is therefore the lowest temperature at which to obtain fast polymerization. Curve 2 corresponds to the dehydration of $La(OH)_3$. The first weight loss (~ 400° C) is associated with intramolecular dehydration and the second, at ~ 500° C, to an

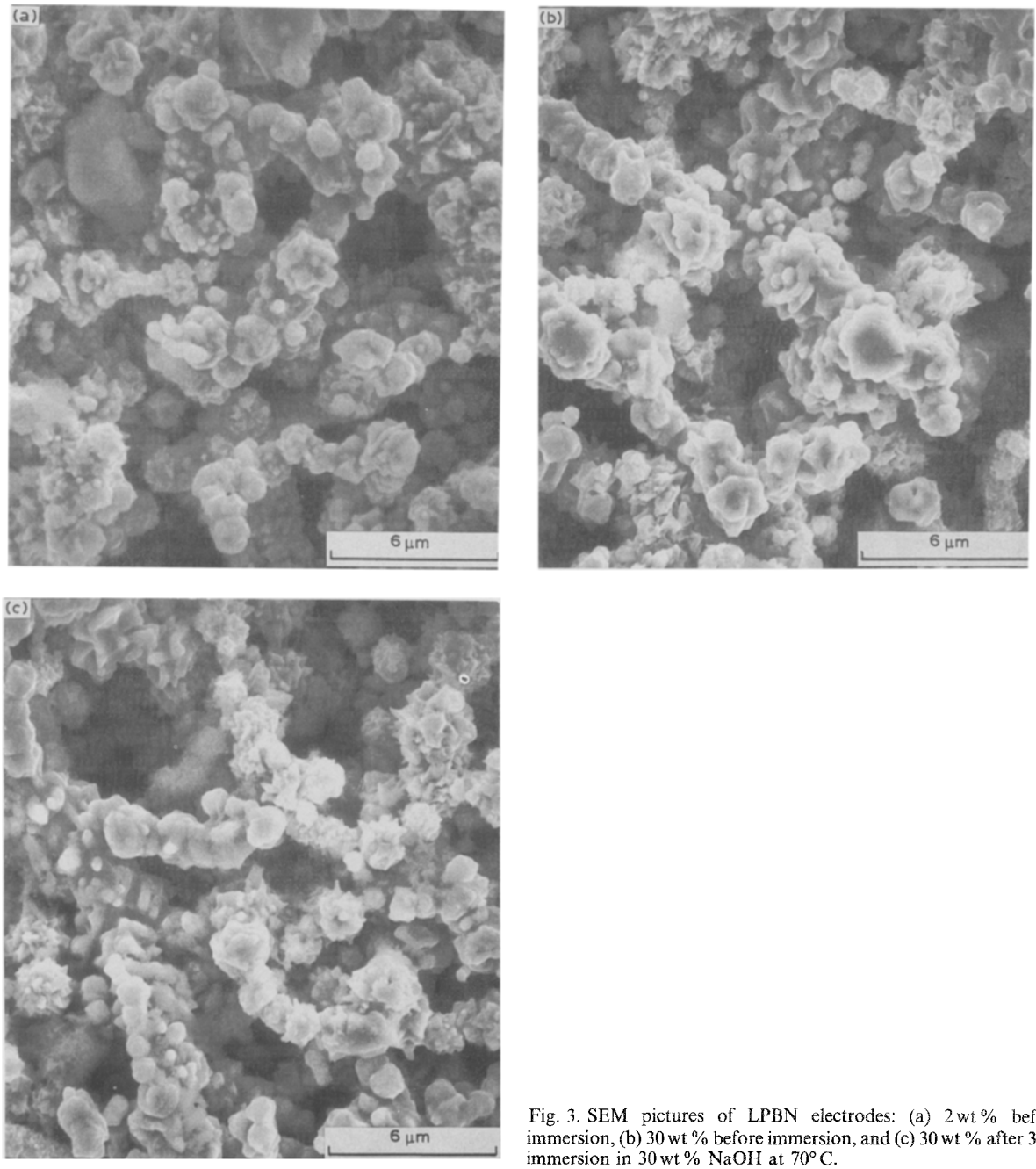

Fig. 3. SEM pictures of LPBN electrodes: (a) 2 wt % before immersion, (b) 30 wt % before immersion, and (c) 30 wt % after 30 h immersion in 30 wt % NaOH at 70° C.

intermolecular reaction resulting in the formation of La_2O_3. Curve 3 is related to the dehydration of $La(H_2PO_4)_3$, which leads to $La(PO_3)_3$ according to the XRD results. Since the latter compound was not observed as a polymerization product, the $LaPO_4$ (monazite) must have been produced by the intermolecular dehydration reaction between $La(H_2PO_4)_3$ and $La(OH)_3$.

The chemical stability of both $LaPO_4$ and $AlPO_4$ was investigated by immersing pellets of pure $LaPO_4$ and $AlPO_4$ in 30 wt % NaOH at 70° C. (Pellets of $AlPO_4$ were prepared according to a procedure described in detail in [5].) Pellets of $LaPO_4$ were not significantly dissolved after several hours of immersion while those of $AlPO_4$ were completely dissolved within few minutes of immersion. It was deduced that $LaPO_4$ is stable in the presence of concentrated alkaline solutions, $AlPO_4$ being very unstable.

The chemical stability of the LPBN electrodes was determined by immersion at o.c.p. in a 30 wt % NaOH solution at 70° C; these experimental conditions are more severe than immersion in 1 M KOH at 25° C. The percentage weight loss against the immersion time is shown in Fig. 2 for LPBN electrodes containing from 2 to 20 wt % binding material. As reported for APBN electrodes [5], the lower the binder content, the lower the weight loss. A large improvement in the chemical stability of the electrode materials is observed when the binding agent is $LaPO_4$. For example, a 10 wt % APBN pellet loses 6 wt % in 30 h, whereas for the same immersion time a 10 wt % LPBN electrode loses only 1.3 wt %. As the amount of binder was increased to 20 wt %, APBN pellets disintegrated after several minutes of immersion; by contrast, LPBN electrodes (20 wt %) were stable and lost only 3.7 wt % after 200 h immersion. It may thus be concluded that the chemical stability of the electrode materials is largely improved when $LaPO_4$ replaces $AlPO_4$ as the binding agent.

SEM recordings (Jeol) of 2 and 30 wt % LPBN electrodes before and after immersion are presented in Fig. 3. The electrodes have practically the same morphology as a result of the cementing process. The surface was very rough with deep pores. The fractal shape of the nickel powder and the porous nature of the electrode material were unchanged, despite the pressure (up to 340 kg cm^{-2}) used in the preparation of the pellets.

3.2. *Hydrogen evolution reaction*

3.2.1. Kinetic parameters. Figure 4 shows Tafel plots for 2 wt % LPBN electrodes. The first polarization curve corresponds to a fresh LPBN electrode while the second was recorded immediately after electrochemical oxidation and the third after stabilization of the Tafel line under cathodic polarization. The Tafel lines for a fresh electrode and an electrode after oxidation and subsequent stabilization are practically the same, although the electrode is slightly more active after stabilization. This behaviour is probably related to the fact that oxides generated during electrochemical oxidation are not completely reduced. The kinetic parameters of the HER after oxidation and subsequent stabilization of the Tafel curves are summarized in Table 1 for LPBN and APBN electrode materials containing different amounts of binding materials. The kinetic parameters of the HER and the overpotentials at 250 mA cm^{-2} are practically the same for the two types of electrode.

Nickel smooth electrodes generally exhibit a Tafel slope of about 120 mV decade^{-1} in alkaline solutions [3, 7–11], at temperatures ranging from 20–80° C [8]. These electrodes have a much lower exchange-current density than LPBN electrodes, which are high surface area pellets. For LPBN electrodes, the real surface area determined by BET analysis is 1.5 m^2 g^{-1} i.e. a

Table 1. Characteristics of phosphate-bonded Ni electrodes (1 M KOH, 25° C)

Metallic composition/wt %	*Chemical stability in alkaline media*	*Electrical resistivity/10^{-5} Ω cm*	*Kinetic parameters of HER**		
			Tafel slope/mV decade^{-1}	*Exchange-current density/mA cm^{-2}*	*Overpotential at 250 mA cm^{-2} mV*
Lanthanum phosphate					
98	good	9.4	112	2.9	217
95	–	11.0	130	3.8	236
90	good	34.0	135	4.4	236
80	good	42.0	128	4.9	219
70	good	56.0	–	–	–
Aluminium phosphate					
98	good	8.9†	120	6.0	191
95	good	–	125	5.3	212
90	poor	24.0†	140	5.8	228
80	poor	15.0†	132	4.5	230
70	poor	24.0†	–	–	–

* From stabilized-polarization curves after electrochemical oxidation.
† From [4]. The electrical resistivity of sintered nickel powder electrodes without binding material is 7.4 × 10^{-5} Ω cm.

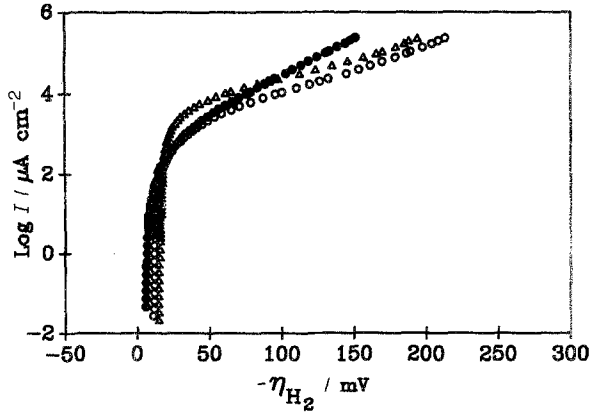

Fig. 4. Tafel curves for HER on 2 wt % LPBN electrodes in KOH 1 M at 25° C: (○) for fresh LPBN electrodes, (●) after electrochemical oxidation, and (△) after stabilization following electrochemical oxidation.

working surface of 3900 cm^2 for 1 cm^2 of geometric surface. Porous nickel electrodes produced by plasma spray [10] and vacuum evaporation [12, 13] exhibit better HER kinetic parameters and a lower overpotential than LPNB electrodes despite the considerable roughness of the latter.

Figure 5 shows the overpotential at 250 mA cm^{-2} plotted against the binder content for the different treatments applied to LPBN electrodes. The electrocatalytic performance towards the HER at 250 mA cm^{-2} is seen to be only slightly affected by the binder content, whereas APBN electrodes show a decrease in activity as the binder content increases (Table 1).

3.2.2. HER overpotential against time. Figure 6 presents η_{H_2} against time for 2 wt % APBN and 5% LPBN electrode (equivalent molar percentage in both cases). In Fig. 6a the η_{H_2} against time behaviour was obtained at 25° C in 1 M KOH at a current density of 100 mA cm^{-2} and the curves show a loss of activity during the first 48 h of polarization for both electrodes. The HER overpotential of LPBN electrodes stabilizes after 48 h of polarization; by contrast, APBN electrodes deactivate during the first 200 h polarization. Figure 6b shows polarization curves in 30 wt % KOH at 70° C for 5 wt % LPBN and 2 wt %

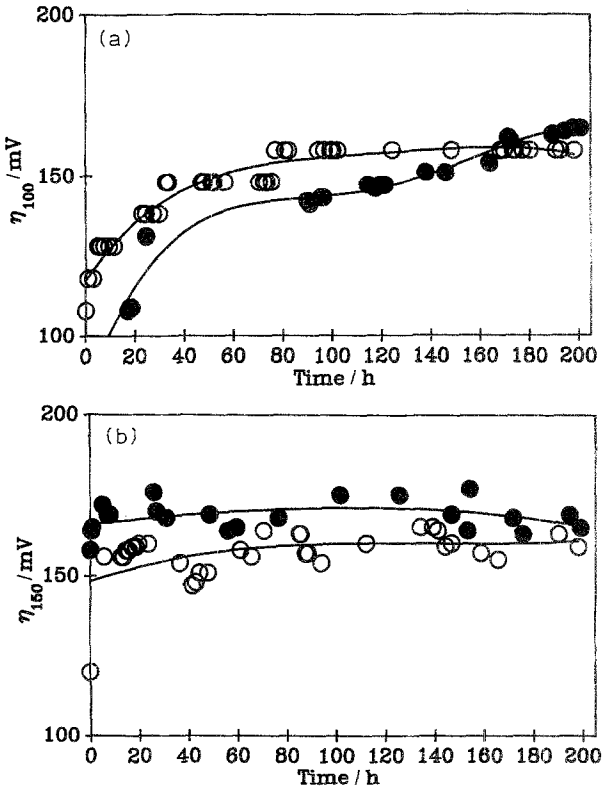

Fig. 6. Overpotential against time for HER on a 2 wt % APNB (●) and 5 wt % LPNB (○) electrodes in KOH. *E* values were corrected for *IR* drop. (a) 100 mA cm^{-2}, 1 M KOH at 25° C, and (b) 150 mA cm^{-2}, 30 wt % KOH at 70° C.

APBN electrodes at a current density of 150 mA cm^{-2}. The overpotential was about 160 mV for both electrodes and a small deactivation was observed in such conditions. The electrocatalytic activity with respect to the HER is approximately the same for both electrodes. In the case of 5 wt % LPBN electrodes, the pressure used for their preparation (80–4000 kg cm^{-2}) does not affect the HER rate (Fig. 7).

3.3. *Oxygen evolution reaction*

A 2 wt % LPBN electrode was polarized under an anodic current density of 250 mA cm^{-2} in 1 M KOH at 25° C for 1–36 h (Fig. 8). Tafel lines were obtained after polarization at 250 mA cm^{-2}; their character-

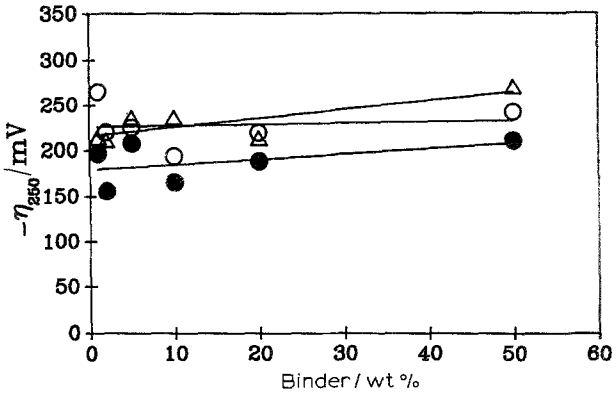

Fig. 5. Overpotential of HER at 250 mA cm^{-2} against binder content for (○) fresh, (●) electrochemically oxidized and (△) stabilized LPBN electrodes. A cathodic current of about 250 mA cm^{-2} was applied for 30 min prior to the η_{H_2} measurements.

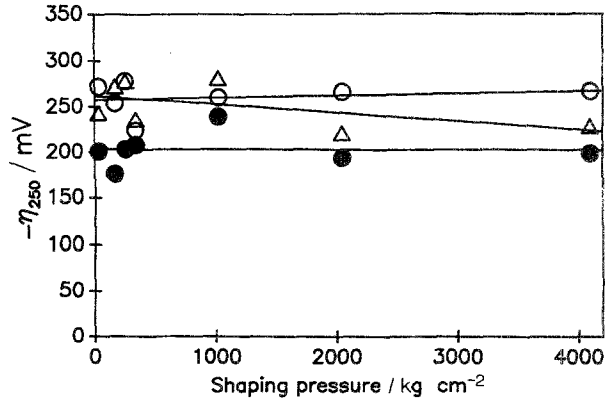

Fig. 7. Effect of pressure applied during electrode preparation on HER overpotential at 250 mA cm^{-2} in KOH 1 M at 25° C (5 wt % LPBN electrode). (○) Fresh, (●) electrochemically oxidized, and (△) stabilized electrode after oxidation.

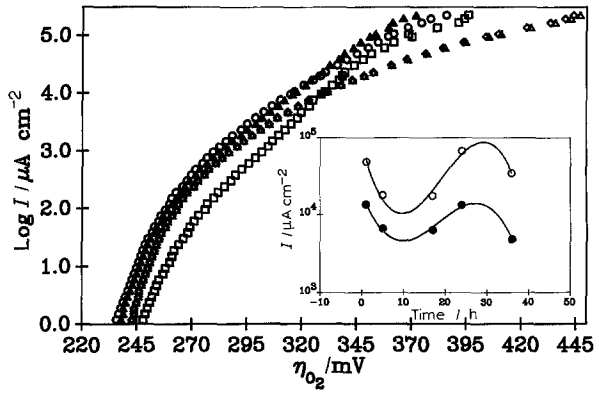

Fig. 8. Polarization curves for OER on 2 wt % LPBN electrode in KOH 1 M at 25° C, for different preanodization time under about 250 mA cm^{-2} (η_{O_2} are *IR*-corrected). Preanodization times: (○) 1 h, (◇) 5 h, (△) 17 h, (▲) 24 h, and (□) 36 h. Insert shows the variation of current against preanodization time at η_{O_2} = 345 mV (○) and η_{O_2} = 320 mV (●).

istics depend on the preanodization time. The anodic current density at η_{O_2} = 320 or 345 mV against polarization time is given in the insert of Fig. 8. The oscillatory behaviour observed is very tentatively related to modifications in the nature of the oxide(s) and/or hydroxide(s) while the exact nature of these modifications are not understood. When the polarization time is long enough, the Tafel lines stabilize. The kinetic parameters for the OER for different $LaPO_4$ contents after Tafel line stabilization are summarized in Table 2. The best performances are observed for 5 wt % binder content, when the Tafel slope reaches its lowest value, 80 mV decade^{-1}. The average slope, 87 mV decade^{-1}, is higher than the value reported by Lu *et al.* [14] for a porous nickel electrode (62 mV decade^{-1}) but the exchange-current density is much higher for porous LPBN electrodes. The kinetic parameters were similar to those reported by Miles *et al.* [9] for smooth electrodes in a more concentrated alkaline medium. Tafel slopes of porous nickel powder electrodes as low as 35 mV decade^{-1} have been reported [16]. No desintegration of the pellets was detected for an anodic polarization time of approximately 50 h.

3.4. *Cyclic voltammetry*

Cyclic voltammograms of the LPBN electrodes were recorded at potentials ranging from OER (800 mV) to HER (− 1200 mV). First the electrodes were subjected to an anodic current of 250 mA cm^{-2}. Then the potential was scanned at 0.01 V s^{-1} in the cathodic direction. The curves were similar in shape and peak location to those reported in the literature for polycrystalline nickel [4, 17] in alkaline aqueous solutions.

4. Conclusion

Lanthanum phosphate can be substituted for aluminium phosphate to cement nickel powders used to produce high surface area electrodes for alkaline water electrolysis. The electrocatalytic activity toward the HER and the electrical conductivity of the electrode materials are only slightly affected by the nature of this phosphate compound, but the chemical stability at the open circuit potential is improved significantly with $LaPO_4$.

Acknowledgment

The National Research Council of Canada, Hydro-Québec and the Quebec government are acknowledged for their financial support. We thank M. L. Timberg of Inco Metals Company for furnishing the characterized nickel powders.

References

[1] C. T. Bowen, H. J. Davis, B. F. Henshaw, R. Lachance, R. L. LeRoy and R. Reynold, *Int. J. Hydrogen Energy* **9** (1984) 59.
[2] K. Lohrberg and P. Kohl, *Electrochim. Acta* **29** (1984) 1557.
[3] A. Lasia and A. Rami, *J. Electroanal. Soc.* **294** (1990) 123.
[4] Y. Choquette, L. Brossard and H. Ménard, *Int. J. Hydrogen Energy* **15** (1990) 551.
[5] E. Potvin, H. Ménard, J. M. Lalancette and L. Brossard, *J. Appl. Electrochem.* **20** (1990) 252.
[6] E. Potvin, A. Lasia, H. Ménard, L. Brossard, *J. Electrochem. Soc.* **138** (1991) 900.
[7] A. C. Makrides, *ibid.* **109** (1962) 977.
[8] H. Kronberger, Ch. Fabjan, and G. Frithum, *Int. J. Hydrogen Energy* **16** (1991) 219.
[9] M. H. Miles, G. Kissel, P. W. T. Lu and S. Srinivasan, *J. Electrochem. Soc.* **123** (1976) 332.
[10] D. E. Hall, *J. Appl. Electrochem.* **14** (1984) 107.
[11] A. C. Mackrides, *J. Electrochem. Soc.* **113** (1966) 1158.
[12] L. Angely, G. Bronoel and G. Peslerbe, *ibid.* **96** (1979) 203.
[13] M. Bica de Moares, D. M. Soares and O. Teschke, *ibid.* **131** (1984) 1931.
[14] P. W. T. Lu and S. Srinivasan, *ibid.* **125** (1978) 265.
[15] D. E. Hall, *ibid.* **128** (1981) 740.
[16] W. Visscher and E. Barendrecht, *Electrochim. Acta* **125** (1980) 651.

Table 2. Electrocatalytical characteristics of OER at 25° C of lanthanum phosphate bonded Ni electrodes (1 M KOH)

Metallic composition/wt %	*Kinetic parameters of OER**		
	Tafel slope/mV decade^{-1}	*Exchange-current density/10^{-3} mA cm^{-2}*	*Overpotential at 250 mA cm^{-2}* mV
Lanthanum phosphate			
98	94	2.80	465
95	80	1.35	422
90	–	–	–
80	84	1.76	430
70	90	3.90	460

* After stabilization at 70° C at an anodic current of 250 mA cm^{-2}.